Regulation of MAPK Function by Direct Interaction with the Mating-Specific Gα in Yeast

Metodi V. Metodiev,[1] Dina Matheos,[2] Mark D. Rose,[2] David E. Stone[1*]

The mating response of the budding yeast *Saccharomyces cerevisiae* is mediated by a prototypical heterotrimeric GTP-binding protein (G protein) and mitogen-activated protein kinase (MAPK) cascade. Although signal transmission by such pathways has been modeled in detail, postreceptor down-regulation is less well understood. The pheromone-responsive G protein α subunit (Gα) of yeast down-regulates the mating signal, but its targets are unknown. We have found that Gα binds directly to the mating-specific MAPK in yeast cells responding to pheromone. This interaction contributes both to modulation of the mating signal and to the chemotropic response, and it demonstrates direct communication between the top and bottom of a Gα-MAPK pathway.

The pheromone response system of *S. cerevisiae*, which enables haploid cells of opposite mating type to sense one another's presence and to differentiate into gametes, uses signaling molecules found in all eukaryotic cells. Upon binding ligand, the pheromone receptor activates its associated heterotrimeric G protein, causing the Gα and Gβγ subunits to dissociate. Gβγ then interacts with a p21-activated protein kinase (PAK) homolog, Ste20, and a scaffolding protein, Ste5, to stimulate a MAPK module composed of Ste11 [the mitogen-activated protein kinase kinase kinase (MEKK)], Ste7 [the mitogen-activated protein kinase kinase (MEK)], and Fus3 (the MAPK). The activated form of Fus3 is thought to translocate to the nucleus (*1*), where it phosphorylates targets that effect changes in gene expression and that block cell-cycle progression (*2*). In addition to stimulating the MAPK cascade, Gβγ is critical for polarized growth toward pheromone (*3*). Although Gβγ plays a positive signaling role, the pheromone-responsive Gα protein, Gpa1, negatively regulates the mating signal (*4*, *5*). In its inactive (GDP-bound) form, Gpa1 couples Gβγ to the receptor. When activated, Gpa1 promotes adaptation to pheromone by mechanisms that have not been well defined, although genetic evidence suggests that Gpa1-GTP down-regulates the mating response by stimulating an unknown protein to interact with Gβγ (*6*) and by antagonizing the function of Fus3 (*7*, *8*).

To identify putative Gpa1 effectors, a glutathione *S*-transferase (GST)–tagged form of Gpa1 was expressed in yeast cells, and glutathione-agarose pull-down experiments were performed (*9*). Copurifying proteins were identified by high-resolution two-dimensional electrophoresis and mass spectrometry. Several polypeptides that bound specifically to the GST-Gpa1 matrix, and not to GST control beads, were recovered [fig. S1 (*9*)]. One of these polypeptides was enriched in the samples derived from cells treated with mating pheromone. After the polypeptides were subjected to in-gel trypsinization and the masses of the resulting fragments determined, a database search revealed that the pheromone-inducible spot was the mating-specific MAPK, Fus3. The pheromone-responsive Gβ moiety, Ste4, was also identified. Thus, GST-Gpa1 precipitated molecules at the top of the pheromone response pathway, as well as downstream in the pathway.

To confirm Gpa1 association with Fus3, an affinity matrix was made with histidine-tagged Gpa1 purified from *Escherichia coli*. A yeast strain was constructed in which the genomic copy of *FUS3* was replaced by a COOH-terminal Myc-tagged form of *FUS3* expressed from its own promoter. This strain was cultured with and without pheromone, and whole-cell lysates were prepared. The Gpa1 affinity matrix

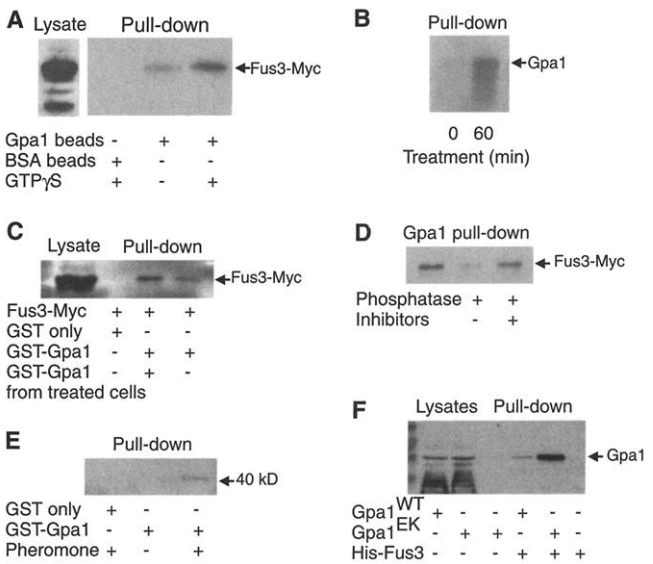

Fig. 1. Biochemical characterization of Gpa1-Fus3 interaction. (**A**) Gpa1 associates with Fus3 in vitro. Whole-cell lysates from yeast cells expressing Fus3-Myc were incubated overnight with the indicated reagents. After extensive washing, the bound proteins were eluted in SDS sample buffer and analyzed by immunoblotting using a polyclonal antibody against Myc. (**B**) Fus3 associates with Gpa1 in vivo. Fus3-Myc immunoprecipitates were probed for the presence of Gpa1 with antibody against Gpa1. The cultures were treated with pheromone as indicated. (**C**) Pheromone-induced activation of Gpa1 increases its association with Fus3. Lysates from pheromone-treated yeast cells expressing Fus3-Myc were incubated overnight with lysates from yeast cells expressing GST or GST-Gpa1, pheromone-treated or not, as indicated. The reactions were precipitated with glutathione (reduced form) (GSH) affinity beads, and the bound proteins probed with Myc-specific antibodies. (**D**) Effect of phosphatase treatment on Gpa1-Fus3 interaction. Yeast cell lysates expressing Fus3-Myc were treated with phosphatase, or phosphatase plus phosphatase inhibitors, and incubated overnight with equal amounts of purified Gpa1, covalently attached to agarose beads. The bound proteins were analyzed by Western blot using a Myc-specific antibody. (**E**) The activated form of Fus3-Myc associates with Gpa1 in vitro. Lysates from pheromone-treated and untreated yeast cells expressing Fus3-Myc were incubated overnight with lysates from yeast cells expressing GST or GST-Gpa1. Gpa1 was precipitated with GSH affinity beads, and the bound proteins were probed with an monoclonal antibody against pTEpY that reacts specifically with the doubly phosphorylated MAPKs. (**F**) Physical association of bacterially expressed Fus3 and Gpa1. A His-tagged form of Fus3 and untagged forms of Gpa1 were expressed in *E. coli*. Equal amounts of the Fus3 and Gpa1 [either wild type (WT) or the mutant $Gpa1^{E364K}$ (EK)] containing lysates were mixed, incubated in the presence of 5 mM $MgSO_4$ and 100 μM GTP-γ-S for 30 min at room temperature, and His-Fus3 was purified on Ni-nitrilotriacetic acid affinity resin. Bound proteins were probed with a polyclonal antibody against Gpa1.

[1]Department of Biological Sciences, Laboratory for Molecular Biology, University of Illinois at Chicago, 900 South Ashland Avenue (M/C 567), Chicago, IL 60607, USA. [2]Princeton University, Department of Molecular Biology, Princeton, NJ 08544, USA.

*To whom correspondence should be addressed. E-mail: dstone@uic.edu

specifically bound Fus3-Myc from cells treated with pheromone (Fig. 1A), but not from untreated cells (*9–11*). Endogenous Gpa1 in lysates from pheromone-treated cells was also coimmunoprecipitated with Fus3-Myc by a Myc-specific antibody (Fig. 1B).

Because pheromone both induces the de novo synthesis of Gpa1 and Fus3 (*12*) and activates their signaling functions (*2*), the pheromone dependence of the Gpa1-Fus3 association could be explained in a number of ways. Two observations suggest that activation of Gpa1 is an important factor. Loading the Gpa1 matrix with GTP-γ-S increased its binding to Fus3-Myc [Fig. 1A and fig. S2 (*9*)]. Also, when lysates from pheromone-treated Fus3-Myc–expressing cells were mixed with lysates from pheromone-treated and untreated GST-Gpa1–expressing cells, the strongest Gpa1-Fus3 interaction was observed with GST-Gpa1 prepared from the pheromone-stimulated cells (Fig. 1C). This effect was not due to increased GST-GPA1, because the tagged Gpa1 was expressed from the *CUP1* promoter, which is not induced by pheromone (*12*). Rather, pheromone most likely increased the Gpa1-Fus3 interaction by activating Gpa1. To distinguish the effects of pheromone-induced activation and pheromone-induced expression of Fus3 lysates containing Fus3-Myc were treated with phosphatase before testing for association with Gpa1. Phosphatase treatment decreased the amount of Fus3-Myc precipitated by Gpa1, indicating that Gpa1 preferentially associates with the phosphorylated (activated) Fus3 (Fig. 1D). In addition, a protein of about the mass of Fus3 was identified by Western blot analysis of Gpa1-associated proteins with an antibody (against pTEpY) that recognizes only activated MAPK (Fig. 1E).

To determine whether Gpa1 can interact directly with Fus3, a histidine-tagged form of Fus3 was purified from *E. coli* on a nickel column and tested for the ability to pull out Gpa1 from a bacterial lysate. Bacterially expressed Gpa1 bound to the bacterially expressed His-Fus3, suggesting that the two proteins can interact directly (Fig. 1F). Phosphatase treatment of the His-Fus3 produced in *E. coli* also decreased its interaction with Gpa1 (*9*, *10*, *13*). In addition, a hyperadaptive mutant form of Gpa1 ($Gpa1^{E364K}$) bound to His-Fus3 considerably better than did wild-type Gpa1 (*14*).

To ascertain the functional significance of the Gpa1-Fus3 interaction, we studied the effect of disrupting it. Recently, a MAPK docking motif was discovered in Ste7, the MEK that directly activates Fus3 (*15*). This motif, LQ_RR_N_LKGLNLNL (*14*), was shown to be necessary and sufficient to bind GST to the yeast MAPKs Fus3 and Kss1 and to their mammalian ortholog, Erk2. A MAPK-binding sequence was identified in

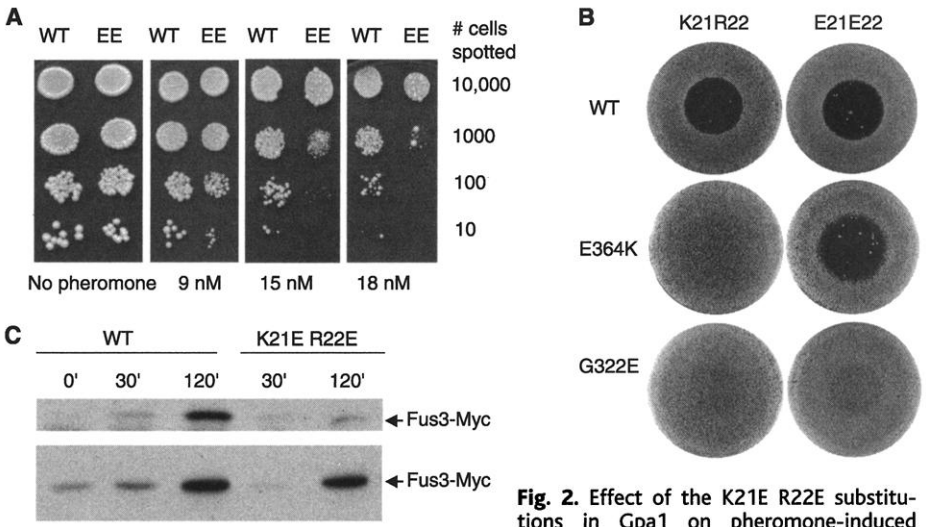

Fig. 2. Effect of the K21E R22E substitutions in Gpa1 on pheromone-induced growth arrest. **(A)** *MATa gpa1Δ* cells transformed with centromeric vectors containing either *GPA1* (WT) or $gpa1^{K21E\ R22E}$ (EE) were grown to stationary phase, diluted, and spotted onto rich medium containing the indicated concentrations of pheromone. **(B)** *MATa gpa1Δ* cells transformed with centromeric vectors containing the indicated alleles of *GPA1* were assayed for pheromone sensitivity in standard halo tests, as previously described (*5*). Top, *GPA1* and $gpa1^{K21E\ R22E}$; center, $GPA1^{E364K}$ and $gpa1^{K21E\ R22E\ E364K}$; bottom, $GPA1^{G322E}$ and $GPA1^{K21E\ R22E\ G322E}$. **(C)** Immunoblot showing the effect of the K21E R22E substitutions in Gpa1 on the Gpa1-Fus3 interaction. Lysates were prepared from pheromone-treated yeast cells expressing Fus3-Myc and either wild-type Gpa1 (WT), or $Gpa1^{K21E\ R22E}$ (EE). Top, Gpa1 immunoprecipitates were probed for the presence of Fus3-Myc; bottom, Fus3-Myc immunoprecipitates were probed for the presence of Fus3-Myc.

Gpa1 (residues 21 to 33) and in four other proteins known to interact with Fus3 (fig. S3). To determine whether the putative Fus3 docking motif is critical for the function of Gpa1, we changed residues lysine 21 and arginine 22 to glutamate in wild-type Gpa1, and in two mutant Gpa1 proteins, $Gpa1^{E364K}$ and $Gpa1^{G322E}$. Although both $Gpa1^{E364K}$ and $Gpa1^{G322E}$ inhibit the mating signal, they do so by distinct mechanisms. $Gpa1^{E364K}$ is an activated form of Gα that promotes hyperadaptation to pheromone, whereas $Gpa1^{G322E}$ is an inactivated form of Gα that confers insensitivity to pheromone (*5*, *16*). The various mutant alleles of *GPA1* were transformed into a *gpa1Δ GAL1-GPA1* strain (*5*), and the expression of wild-type Gpa1 was turned off. All mutant forms of Gpa1 conferred normal growth to cells lacking wild-type Gpa1, indicating that the K21E R22E double-mutation does not disrupt Gα-Gβγ binding (Fig. 2, A and B). In contrast, mutation of the putative Fus3 docking site did compromise the ability of Gpa1 to promote adaptation to pheromone. Cells expressing $Gpa1^{K21E\ R22E}$ exhibited enhanced sensitivity to pheromone-induced cell-cycle arrest in assays of single-colony formation (Fig. 2, A and B) (*17*), and unlike $Gpa1^{E364K}$, $Gpa1^{K21E\ R22E\ E364K}$ conferred only very modest hyperadaptivity (Fig. 2B). The G322E mutant form of Gpa1, which is thought to confer resistance to pheromone by sequestering Gβγ, was largely unaffected by the K21E R22E mutation. As expected, the binding of $Gpa1^{K21E\ R22E}$ to Fus3-Myc in vivo was impaired (Fig. 2C).

The inverse correlation between Gpa1-Fus3 interaction and Gpa1-mediated adaptation is consistent with the idea that Gpa1 directly inhibits Fus3 signaling. Gpa1 could anchor Fus3 in the cytoplasm and prevent communication of the mating signal to the nucleus. Consistent with this possibility, we have found that $Gpa1^{E364K}$ reduces the localization of a Fus3-GFP reporter to the nuclei of cells responding to pheromone (*10*). Gpa1 could also target Fus3 for degradation, as activated Gpa1 is subject to regulated degradation by the N-end rule pathway (*18*), and the Gpa1-Fus3 interaction might mark the kinase for the same fate. Gpa1 might also inhibit the catalytic function of Fus3. Fus3 kinase activity was inhibited in vitro by wild-type Gpa1 equilibrated with GTP-γ-S, but was unaffected by inactive (GDP-bound) Gpa1 [fig. S2 (*9*)]. $Gpa1^{E364K}$ inhibited Fus3 activity when equilibrated with either GDP or GTP, consistent with its hyperadaptive activity. Although these results do not necessarily reflect the effect of Gpa1 on Fus3 activity in vivo, they argue against the possibility that Gpa1 stimulates Fus3. In contrast, the binding of mammalian Gα proteins to tyrosine kinases induces kinase activity (*19–22*).

In addition to down-regulating the cell-cycle inhibitory effect of Fus3, we considered the possibility that Gpa1-Fus3 interaction plays a positive role in mating. When placed in a physiological gradient of pher-

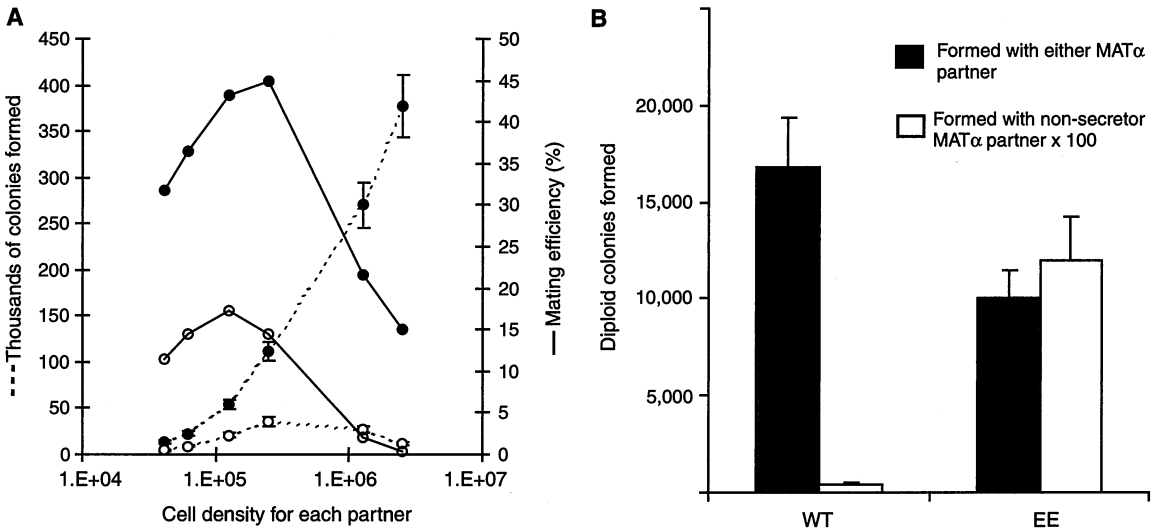

Fig. 3. Effect of *gpa1*$^{K21E\ R22E}$ on mating efficiency and fidelity. (**A**) Quantitative bilateral mating assays were performed. Open symbols correspond to the mutant cells; closed symbols correspond to the wild-type cells. (**B**) Mating partner discrimination assays were performed with wild-type (WT) and *gpa1*$^{K21E\ R22E}$ (EE) strains.

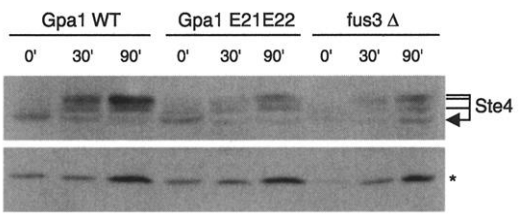

Fig. 4. Effect of *gpa1*$^{K21E\ R22E}$ and *fus3*Δ on the phosphorylation and level of Ste4. Wild-type, *gpa1*$^{K21E\ R22E}$, and *fus3*Δ cells were grown to mid-log phase, and treated with 60 nM pheromone. Samples were taken at the indicated times and analyzed by electrophoresis and immunoblotting. The blot was probed with affinity-purified Ste4 antibody. The arrow marks the position of unphosphorylated Ste4, and the lines indicate the phosphorylated forms. The asterisk marks an unknown protein that cross-reacts with the Ste4 antibody.

omone, yeast cells reorganize their cytoskeletons and polarize their growth in the direction of highest concentration of ligand. This phenomenon is called chemotropism: mating partners grow toward one another and eventually fuse at their tips. Gpa1 and Far1, a substrate of Fus3, have been implicated in the chemotropic response (*3*, *23*), and Fus3 is required for cell fusion (*24*). Moreover, both Gpa1 and Fus3 concentrate at the tips of the mating projections [fig. S4 (*9*)]. If Gpa1 serves to localize Fus3 to the sites of polarized growth, and if Fus3 must get to these sites to promote chemotropism and/or cellular fusion, then we would expect the K21E R22E allele of *GPA1* to confer a defect in mating. Indeed, *gpa1*$^{K21E\ R22E}$ cells mated with about 1/15th the efficiency of isogenic cells expressing wild-type *GPA1* (Fig. 3A). The mutant cells also exhibited a defect in chemotropism: When challenged with a mixture of pheromone-secreting and nonsecreting mating partners, the mutant cells were about 50 times more likely than wild-type cells to mate with the nonsecretors (Fig. 3B). These results suggest that wild-type mating efficiency depends on the interaction between Fus3 and Gpa1, and that the mating defect conferred by *gpa1*$^{K21E\ R22E}$ is partially due to the decreased ability of the mutant cells to orient toward their mating partners.

Ste4 is rapidly phosphorylated on multiple sites in cells responding to pheromone, and this is partially dependent on Fus3 (*25*) and Gpa1 (*26*). Moreover, the Gβγ-Far1 complex is thought to mark the site of chemotropic growth. Therefore, we tested the effect of the K21E R22E substitutions in Gpa1 on the fate of Ste4 after pheromone stimulation. Two mutants, *gpa1*$^{K21E\ R22E}$ and *fus3*Δ (*25*), decreased the phosphorylation and the level of Ste4 in stimulated cells (Fig. 4). Moreover, a mutant form of Ste4 that cannot be phosphorylated (Ste4$^{T320A\ S335A}$) conferred a defect in chemotropism similar in magnitude to that caused by *gpa1*$^{K21E\ R22E}$ (*10*). One way to explain these findings is to postulate that in cells exposed to a physiological gradient of pheromone, Gpa1 recruits Fus3 to the incipient mating projection site. There, the kinase phosphorylates Ste4, which promotes assembly or stabilization of the Gβγ-Far1 complex required for chemotropic growth.

To date, heterotrimeric G protein and MAPK signaling pathways have been modeled as linear. However, the pheromone-responsive Gα protein at the top of the yeast mating pathway interacts directly with the MAPK at the end of the pathway. This interaction may serve two seemingly contradictory purposes: The supersensitive or adaptive-negative phenotype conferred by disruption of Gpa1-Fus3 interaction suggests that Gpa1 promotes adaptation to pheromone by down-regulating Fus3, whereas the mating and/or chemotropic defects conferred by disruption of Gpa1-Fus3 interaction suggest that Gpa1 potentiates the function of Fus3 in polarization and/or conjugation. How might Gpa1 act as both a negative and a positive regulator of Fus3? Gpa1 may recruit Fus3 to the sites of polarized growth in mating projections where the kinase phosphorylates targets involved in chemotropism and cell fusion. In so doing, Gpa1 diverts Fus3 away from the nucleus, thereby modulating the intensity and duration of the mating response. Given the structural conservation of G proteins and MAPKs, as well as the conservation of their functional relationships, other examples of Gα-MAPK interactions are possible. In fact, sequences similar to the MAPK docking motif found in Ste7 and Gpa1 are present near the NH_2-termini of the mammalian Gα proteins Golf, Gq, G13, and G14 (fig. S3).

References and Notes

1. K.-Y. Choi, J. E. Kranz, S. K. Mahanty, K.-S. Park, E. A. Elion, *Mol. Biol. Cell* **10**, 1553 (1999).
2. M. C. Gustin, J. Albertyn, M. Alexander, K. Davenport, *Microbiol. Mol. Biol. Rev.* **62**, 1264 (1998).
3. K. Schrick, B. Garvik, L. H. Hartwell, *Genetics* **147**, 19 (1997).
4. I. Miyajima, K. Arai, K. Matsumoto, *Mol. Cell. Biol.* **9**, 2289 (1989).
5. H. F. Stratton, J. Zhou, S. I. Reed, D. E. Stone, *Mol. Cell. Biol.* **16**, 6325 (1996).
6. E. Li, E. Meldrum, H. Stratton, D. E. Stone, *Genetics* **148**, 947 (1998).
7. K. Doi *et al.*, *EMBO J.* **13**, 61 (1994).
8. J. Zhou, M. Arora, D. E. Stone, *Cell Biochem. Biophys.* **30**, 193 (1999).
9. Materials and methods are available as supporting material on *Science* Online.
10. D. Stone, unpublished observations.
11. The affinity of the Gpa1-Fus3 interaction must be high, as the complex remained bound to the affinity support after extensive washing with high salts and detergents. It is also apparent that the Gpa1-Fus3 association requires the NH_2-terminus of Fus3: Truncated forms of Fus3 that retained the COOH-terminal Myc tag were abundant in the lysate, but did not bind to the Gpa1 affinity matrix.

12. C. J. Roberts *et al.*, *Science* **287**, 873 (2000).
13. Fus3 is known to autophosphorylate and autoactivate (*7*), as is the Erk2 MAPK (*28*).
14. J. Bardwell, L. J. Flatauer, K. Matsukuma, J. Thorner, L. Bardwell, *J. Biol. Chem.* **276**, 10374 (2001).
15. Single-letter abbreviations for the amino acid residues are as follows: A, Ala; C, Cys; D, Asp; E, Glu; F, Phe; G, Gly; H, His; I, Ile; K, Lys; L, Leu; M, Met; N, Asn; P, Pro; Q, Gln; R, Arg; S, Ser; T, Thr; V, Val; W, Trp; and Y, Tyr.
16. M. J. Cismowski, M. V. Metodiev, E. M. Draper, D. E. Stone, *Biochem. Biophys. Res. Commun.* **284**, 247 (2001).
17. The halos formed by *gpa1*$^{K21E\ R22E}$ cells were reproducibly 2 mm larger than those formed by wild-type cells.
18. K. Madura, A. Varshavsky, *Science* **265**, 1454 (1994).
19. K. Bence, W. Ma, T. Kozasa, X. Y. Huang, *Nature* **389**, 296 (1997).
20. Y. Jiang *et al.*, *Nature* **395**, 808 (1998).
21. Y.-C. Ma, J. Huang, S. Ali, W. Lowry, X.-Y. Huang, *Cell* **102**, 635 (2000).
22. C. S. Shi, S. Sinnarajah, H. Cho, T. Kozasa, J. H. Kehrl, *J. Biol. Chem.* **275**, 24470 (2000).
23. R. Dorer, P. M. Pryciak, L. H. Hartwell, *J. Cell Biol.* **131**, 854 (1995).
24. H.-A. Fujimura, *J. Cell Sci.* **107**, 2617 (1994).
25. E. Li, M. J. Cismowski, D. E. Stone, *Mol. Gen. Genet.* **258**, 608 (1998).
26. G. M. Cole, S. I. Reed, *Cell* **64**, 703 (1991).
27. S. Offermanns, V. Mancino, J.-P. Revel, M. I. Simon, *Science* **275**, 533 (1997).
28. F. A. Gonzalez, D. L. Raden, M. Rigby, R. J. Davis, *FEBS Lett.* **304**, 170 (1992).
29. We thank S. Reed and L. Hartwell for plasmids, A. Ellicott and H.-j. Kim for technical assistance, S. Zaichick for the photomicrographs, and Nava Segev and Holly Stratton for critical reading of the manuscript. Supported by grants from the American Cancer Society and NSF (D.E.S.)

Supporting Online Material
www.sciencemag.org/cgi/content/full/296/5572/1483/DC1
Materials and Methods
Figs. S1 to S4

4 February 2002; accepted 5 April 2002

Induction of Cachexia in Mice by Systemically Administered Myostatin

Teresa A. Zimmers,[1]* Monique V. Davies,[2] Leonidas G. Koniaris,[1]* Paul Haynes,[2]† Aurora F. Esquela,[1] Kathy N. Tomkinson,[2] Alexandra C. McPherron,[1] Neil M. Wolfman,[2] Se-Jin Lee[1]‡

Mice and cattle with genetic deficiencies in myostatin exhibit dramatic increases in skeletal muscle mass, suggesting that myostatin normally suppresses muscle growth. Whether this increased muscling results from prenatal or postnatal lack of myostatin activity is unknown. Here we show that myostatin circulates in the blood of adult mice in a latent form that can be activated by acid treatment. Systemic overexpression of myostatin in adult mice was found to induce profound muscle and fat loss analogous to that seen in human cachexia syndromes. These data indicate that myostatin acts systemically in adult animals and may be a useful pharmacologic target in clinical settings such as cachexia, where muscle growth is desired.

Myostatin [growth/differentiation factor-8 (GDF-8)] is a transforming growth factor-β (TGF-β) family member that is essential for proper regulation of skeletal muscle mass (*1*). Myostatin is expressed almost exclusively in cells of the skeletal muscle lineage, from embryonic myotome to striated muscle in adults. Mice carrying a targeted deletion of the gene encoding myostatin (*Mstn*) have a dramatic and widespread increase in muscle mass, suggesting that myostatin normally acts as a negative regulator of muscle growth. Individual muscles of *Mstn*$^{-/-}$ mice weigh ~100 to 200% more than those of control animals as a result of muscle fiber hypertrophy and hyperplasia. Although myostatin does not appear to be essential for either viability or fertility, *Mstn* has been remarkably well conserved through evolution; human, rat, murine, porcine, turkey, and chicken myostatin protein sequences are identical in the biologically active COOH terminus of the protein (*2*). The function of myostatin also appears to have been conserved, as *Mstn* mutations in cattle cause the double-muscling phenotype (*2–5*). Because the myostatin loss-of-function phenotype could result entirely from lack of myostatin activity during embryonic development, the role that myostatin plays in adult animals is unknown.

To determine whether myostatin acts in an endocrine fashion in adult mice, we sought to identify myostatin in serum. Myostatin is synthesized as a pre-proprotein activated by two proteolytic cleavages. Removal of the signal sequence is followed by cleavage at a tetrabasic processing site, resulting in a 26-kD NH_2-terminal propeptide and a 12.5-kD COOH-terminal peptide, a dimer of which is the biologically active portion of the protein. Western blot analysis revealed a 12.5-kD protein in the serum of wild-type but not *Mstn*$^{-/-}$ mice that comigrated with purified recombinant myostatin (Fig. 1A).

Next, we measured myostatin activity in

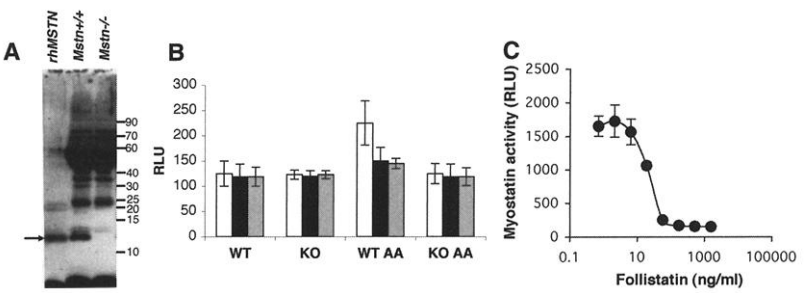

Fig. 1. Detection of myostatin protein and activity. (**A**) Recombinant myostatin (rhMSTN) and serum samples (5 μl) from wild-type (*Mstn*$^{+/+}$) and *Mstn*$^{-/-}$ mice were subjected to SDS–polyacrylamide gel electrophoresis (SDS-PAGE) under reducing conditions. Western blot analysis was then performed with the use of a rabbit polyclonal antiserum raised against bacterially expressed recombinant myostatin COOH-terminal protein. Location of myostatin COOH-terminal monomer is indicated by arrow. Higher molecular weight bands were also detected in the serum of both wild-type and knockout mice, including a clear band around 25,000. Similar nonspecific bands may have given rise to the identification in other reports of a 26-kD "myostatin-related protein" in the blood (*27*) and muscle (*27–31*) of mice and humans. (**B**) A204 assay (*6*) of serum myostatin activity in normal and acid-activated (AA) wild-type (WT) and *Mstn*$^{-/-}$ (KO) serum samples, in the presence of no added factor (white bars), 500 ng/ml propeptide (black bars), or 500 ng/ml follistatin (gray bars). Such data, in comparison to standard curves generated with recombinant myostatin diluted in serum (fig. S1; see Materials and Methods in SOM), led us to estimate the concentration of mouse serum myostatin to be around 80 ng/ml. (**C**) Inhibition of 5 ng/ml recombinant COOH-terminal myostatin in the A204 assay by preincubation with follistatin. RLU, relative luciferase units. Error bars are ± SD.

[1]Department of Molecular Biology and Genetics, Johns Hopkins School of Medicine, 725 North Wolfe Street, Baltimore, MD 21205, USA. [2]Wyeth Research Division, Wyeth Pharmaceuticals, Inc., 87 CambridgePark Drive, Cambridge, MA 02140, USA.

*Present address: Department of Surgery, University of Rochester School of Medicine and Dentistry, 601 Elmwood Avenue, Box SURG, Rochester, NY 14642, USA.

†Present address: Torrey Mesa Research Institute, 3115 Merryfield Row, San Diego, CA 92121, USA.

‡To whom correspondence should be addressed. E-mail: sjlee@jhmi.edu